Chemical Engineering Journal 150 (2009) 223–230

Contents lists available at ScienceDirect

Chemical Engineering Journal

journal homepage: www.elsevier.com/locate/cej

Dynamic modelling of glucose oxidation with palladium catalyst deactivation in multifunctional CSTR: Benefits of periodic operation

Zuzana Gogová, Jiří Hanika*

Institute of Chemical Process Fundamentals of the ASCR, v.v.i., Rozvojova 135/2, 165 02 Prague 6, Czech Republic

ARTICLE INFO

Article history:
Received 2 December 2008
Received in revised form 17 February 2009
Accepted 18 February 2009

Keywords:
Glucose oxidation
Palladium catalyst
Reactivation
CSTR
Periodic operation

ABSTRACT

Heterogeneously catalyzed oxidation of glucose in liquid phase was studied as a model reaction under conditions of reversible deactivation of a palladium catalyst. The proposed kinetics model fitted the experimental data very well. The model was used to explore benefits of a CSTR operation under forced periodic modulation of the gas feed stream. The periodic modulation makes it possible to optimize the catalyst reaction–reactivation processes in CSTR, so that the highest possible reactor productivity could be achieved for given input parameters. Under such operation of the multifunctional CSTR, the catalyst activity is long-term steady. Based on simulations, conditions of the highest possible CSTR productivity were identified for given operational parameters.

1. Introduction

In many practical applications gas–liquid reactions are catalyzed by a heterogeneous catalyst. Such reactions usually take place in a three-phase slurry reactor. A good example of such reaction systems are oxidations with oxygen, catalyzed by transient metals like wet air oxidation of pollutants in waste waters, production of chemical specialities, etc.

Glucose (Glc) oxidation with oxygen to gluconic acid (Glcac) is the model reaction in this study. It runs in an alkaline aqueous solution and it is catalyzed by palladium on activated carbon commercial catalyst. This oxidation itself is interesting from the viewpoint of the reaction product utilization in food, pharmaceutical, textile and other industrial fields.

The research interest is mainly focused on several methods of Glcac production (or structures similar to Glcac) – catalytic oxidation [1–8], fermentation techniques [9–12] or enzymatic oxidation [13,14]. The biotechnological routes of Glcac production currently prevail over the catalytic one on an industrial scale. Glc oxidation by oxygen using noble metal catalysts runs selectively at ambient conditions. This fact makes this catalytic process attractive for research. Its problem, on the other hand, is fast deactivation of the catalyst during the reaction course. The deactivation was proved reversible [3].

There are two major reasons behind the catalyst deactivation. First, in diffusion regime the rate limiting step of the process is oxygen transport towards the catalyst surface. The deactivation is caused by a strong adsorption of the substrate degradation products that block the catalyst active centres [2,4]. On the other hand, in kinetic regime where the reaction runs in excess of oxygen, the catalyst deactivation results from formation of metal-oxide phases [15–17]. They are less active compared to chemisorbed oxygen (oxygen adsorbed above the first metallic layer), and so will be referred to as those responsible for change in the catalyst activity. In the case of palladium catalysts this deactivation proceeds very quickly. However, to overcome the deactivation effect is challenging and interesting research task.

A classical approach to overcome the catalyst activity problem leads through the catalyst optimization. Earlier studies reported on beneficial effect of doping the Pt-group metals with promoters, such as Bi or Pb, that improve selectivity and the catalyst resistance to overoxidation [4]. Lifetime of the catalyst remained a problem, though, because of the promoters leaching under the reaction conditions. Recently, very good activity, selectivity and long-term stability were reported for supported gold catalysts [6–8].

Another approach to solve the problems with the catalyst activity deals with the process or reactor optimization. Beneficial effects of composition modulation on a CSTR performance are presented here. In the CSTR, the catalytic process is accompanied by fast reversible catalyst deactivation. We analyzed possibilities of the multifunctional CSTR performance enhancement by optimization

Abbreviations: CSTR, continuous stirred tank reactor; GLR, gas-lift reactor; LHHW, Langmuir–Hinshelwood–Hougen–Watson (kinetics); SSTR, semi-continuous stirred tank reactor.

* Corresponding author. Tel.: +420 2 20390349; fax: +420 2 20920661.
E-mail address: hanika@icpf.cas.cz (J. Hanika).

1385-8947/$ – see front matter © 2009 Elsevier B.V. All rights reserved.
doi:10.1016/j.cej.2009.02.020

Nomenclature

*	vacant catalytic site
a	relative activity
c	concentration in liquid phase (mol m^{-3})
$\bar{c}$	concentration vector
C	specific concentration of catalytic sites (mol kg$_{cat}^{-1}$)
D	diameter (m)
H	height (m)
k	rate constant (see Table 4)
K	adsorption coefficient (see Table 4)
k_La	volumetric mass transfer coefficient (s^{-1})
p	pressure (kPa)
P	period $P = t_R + t_A$ (s)
R_w	specific rate of formation/consumption (mol kg^{-1} s^{-1})
S	split $S = t_R/(t_R + t_A)$
t	time (s)
T	temperature (K)
U	superficial velocity (m s^{-1})
V	volume (m^3)
x	impeller blade thickness (m)
X	conversion (%)
Y	molar fraction in gas phase

Greek symbols

α	active fraction
$\dot{\xi}_w$	specific reaction rate (mol kg^{-1} s^{-1})
θ	fractional coverage
ν	stoichiometric coefficient
ρ_c	catalyst concentration (kg m^{-3})

Subscript/superscript

0	initial, at $t = 0$ s
–	average
*	saturated; vacant site
A	activation/reactivation
ad	adsorbed
ch	chemisorption site
D	deactivation
f	feed
G	gas phase; glycol
Glc	glucose
Glcac	gluconic acid
L	liquid phase
M	mixer
O	oxygen
opt.	optimal
p	physisorption site
R	reaction; reactor (in Eq. (15))
so	inactive oxygen species
tot	total
x	inactive site

of its periodic operation. The catalyst reaction and reactivation times are optimized here through periodic modulation of the CSTR gas feed stream. The aim was to find conditions of the highest possible reactor productivity for given input parameters. For any input parameters, trajectory of the maximum CSTR productivity can be found.

In general, the term "periodic operation" refers to operation regimes in which one or more reactor parameters vary in time. Modulation of mostly composition and/or feed flow rate was researched, e.g. [18–22], with the aim to improve chemical reactors performance through forcing the reactor to operate under transient rather than steady-state conditions. For a process similar to the model one, Markusse et al. found that the catalyst activity can be maintained steady by periodically switching between oxygen and nitrogen flow to the reactor [2]. Silveston in his monograph [23] pays attention to several processes operated in various periodic modes. In this light, optimization analysis of the model system is presented in this paper.

2. Theoretical part

2.1. Kinetics model formulation

Kinetic model was formulated for the model reaction of Glc selective oxidation towards Glcac over the Pd/C catalyst. The kinetic model was selected by best fitting the experimental data. The model was derived from the proposed mechanism, summarized in Table 1. It leans on earlier studies [3,4] and on our own observations and analyses. It assumes that: (i) oxygen is bound on the catalyst active sites in form of O–, (ii) surface reaction is the rate determining step, (iii) three types of active sites are present on the catalyst surface, (iv) only one molecule is adsorbed per one active site.

According to the proposed mechanism, oxygen is adsorbed dissociatively on the catalyst (Table 1, step 2). Physisorption of glucose is followed by hydration to give geminal diol (steps 1 and 3, respectively). The latter is subsequently transformed into gluconic acid by the surface reaction (step 4). One more vacant chemisorption site is needed for this step to proceed. Desorption of the product, Glcac, is facilitated by its neutralisation (step 5).

The mechanism outlined in Table 1 assumes that the catalyst deactivation results from formation of less active oxidic phases (referred to as inactive oxygen species) at the topmost and subsurface Pd layers (step 6) in oxygen-rich conditions. The catalyst reactivation takes place in oxygen-free conditions by transformation of the inactive oxygen species into chemisorbed oxygen (step 7), which is in turn consumed in the main reaction (step 4).

The rate equation (1) in connection with Eq. (2) forms the kinetics model. Eq. (2) emerges from the steps 6 and 7 of Table 1 on assumption that the total specific amount of inactive sites equals the total specific amount of the sites for chemisorption. Eq. (2) describes change in the catalyst activity through a change in fractional coverage by inactive oxygen species, θ_{so}.

$$\dot{\xi}_w = \frac{k_w c_{Glc}\sqrt{c_O}(1-\theta_{so})^2}{(1 + K_{Glc}c_{Glc} + K_{Glcac}c_{Glcac})(1 + K_O\sqrt{c_O})^2} \quad (1)$$

$$\frac{d\theta_{so}}{dt} = \rho_c V_L \left(\frac{k_D\sqrt{c_O}(1-\theta_{so})^2}{(1 + K_O\sqrt{c_O})} - \frac{k_A\theta_{so}(1-\theta_{so})}{(1 + K_O\sqrt{c_O})} \right) \quad (2)$$

where

$$\theta_{so} = \frac{C_{so}}{C_{ch,tot}} \quad (3)$$

Expressions for the lumped rate and adsorption constants of Eqs. (1) and (2) are listed in Table 4.

Relative activity of the catalyst at time t is defined as the ratio of the reaction rate at time t and reaction rate on a fresh catalyst at the same concentrations and temperature:

$$a(t) = \frac{\dot{\xi}_w(t)}{\dot{\xi}_w^0} \quad [T, \bar{c}] = const. \quad (4)$$

Thus the relative activity is useful parameter that characterizes changes in the reaction rate as the catalyst deactivates, and it is obtained conveniently from the experimental results. Eq. (4) applies to all deactivation processes, no matter if the rate equation is separable or not according to the concept of separability [24,25].

Table 1
Elementary steps sequence of the proposed mechanism for the model reaction of Glc oxidation with the catalyst deactivation and reactivation.

	Rate and balance equations
Elementary steps on the catalyst surface	
1 R–COH + $*_p$ ↔ R–COH$_{ad}$	$C_{Glc} = K_1 c_{Glc} C_{*p}$
2 (1/2)O_2 + $*_{ch}$ ↔ O_{ad}	$C_O = K_2 \sqrt{c_O} C_{*ch}$
3 R–COH$_{ad}$ + H_2O ↔ R–CH(OH)$_{2,ad}$	$C_G = K_3 C_{Glc}$
4 R–CH(OH)OH_{ad} + O_{ad} + $*_{ch}$ → R–C(OH)O_{ad} + H_2O + 2$*_{ch}$	$\dot{\xi}_{w,4} = k_{w,4} C_G C_O C_{*ch}$
5 RCOOH_{ad} + OH^- ↔ $RCOO^-$ + H_2O + $*_p$	$C_{Glcac} = K_5 c_{Glcac} C_{*p} / c_{OH^-}$
The catalyst deactivation and reactivation steps	
6 O_{ad} + $*_x$ → ox + $*_{ch}$	$\dot{\xi}_{w,6} = k_{w,6} C_O C_{*x}$
7 ox + $*_{ch}$ → O_{ad} + $*_x$	$\dot{\xi}_{w,7} = k_{w,7} C_{so} C_{*ch}$
The catalyst sites balances	
Physisorption sites	$C_{p,tot} = C_{*p} + C_{Glc} + C_{Glcac} + C_G$
Chemisorption sites	$C_{ch,tot} = C_{*ch} + C_O + C_{so}$
Inactive sites	$C_{x,tot} = C_{*x} + C_{so}$

A rate equation is separable if it can be expressed as a product of two terms – the reaction rate on the fresh catalyst and the catalyst activity in the following form:

$$\dot{\xi}_w = \dot{\xi}_w^0(\bar{c}) a(\alpha) \quad [T] = const. \tag{5}$$

Active fraction α is defined as the ratio of the number of active sites per unit mass of the catalyst and the number of all sites, i.e.:

$$\alpha = \frac{C_{ch,tot} - C_{so}}{C_{ch,tot}} = \frac{1 - \theta_{so}}{1} \tag{6}$$

The rate equation (1) is separable. Combining Eqs. (1), (5) and (6) gives the following relation between the catalyst activity and the active fraction:

$$a = (1 - \theta_{so})^2 = \alpha^2 \tag{7}$$

Thus the activity depends only on the amount of inactive oxygen species. The activity change in Eqs. (1) and (2) comes from the following relation:

$$-\frac{d\alpha}{dt} = \frac{d\theta_{so}}{dt} \tag{8}$$

2.2. Mathematical model of the batch reactor

All the experiments were carried out in semi-continuous stirred tank reactor, SSTR (see the next chapter). Inlet and outlet concentrations of oxygen in the SSTR gas streams were assumed identical. Therefore the SSTR mathematical model consists of liquid phase material balances only Eqs. (9)–(13).

$$\frac{dc_{Glc}}{dt} = -\rho_c \frac{k_w c_{Glc} \sqrt{c_O} (1 - \theta_{so})^2}{(1 + K_{Glc} c_{Glc} + K_{Glcac} c_{Glcac})(1 + K_O \sqrt{c_O})^2} \tag{9}$$

$$\frac{dc_{Glcac}}{dt} = -\frac{dc_{Glc}}{dt} \tag{10}$$

$$\frac{dc_O}{dt} = k_L a (c_O^* - c_O) - \frac{1}{2} \rho_c \frac{k_w c_{Glc} \sqrt{c_O} (1 - \theta_{so})^2}{(1 + K_{Glc} c_{Glc} + K_{Glcac} c_{Glcac})(1 + K_O \sqrt{c_O})^2} \tag{11}$$

$$\frac{d\theta_{so}}{dt} = \rho_c V_L \left(\frac{k_D \sqrt{c_O} (1 - \theta_{so})^2}{(1 + K_O \sqrt{c_O})} - \frac{k_A \theta_{so} (1 - \theta_{so})}{(1 + K_O \sqrt{c_O})} \right) \tag{12}$$

with initial conditions:

$$t = 0 \quad c_{Glc} = c_{Glc}^0 \quad c_O = c_O^0 \quad c_{Glcac} = c_{Glcac}^0 \quad \theta_{so} = \theta_{so}^0 \tag{13}$$

Value of $k_L a$ was for the experimental reactor calculated from correlation (14) [26], derived for oxygen (or air)–water system (coalescing system).

$$k_L a = 6.64 \times 10^{-3} p_V^{0.675} U_G^{0.494} \tag{14}$$

The total power input per unit volume of liquid, p_V, was adjusted for geometry of the experimental reactor by using power number, N_P, obtained from correlation (15) [27]:

$$N_P = 2.5 \left(\frac{x}{D_M} \right)^{-0.2} \left(\frac{D_R}{1000} \right)^{0.065} \tag{15}$$

Oxygen saturation concentration in the liquid phase, c_O^*, was calculated according to data on oxygen solubility in Glc aqueous solutions [28] by using the following regression equation:

$$c_O^* = p(O_2)(1.1624 \times 10^{-5} - 2.3799 \times 10^{-8} (c_{Glc} + c_{Glcac})^{0.6907}) \tag{16}$$

Simulations of reactors provided in this paper were run using commercial software Matlab.

3. Experimental

3.1. The model reaction kinetics study

The model reaction kinetics was studied in the lab-scale semi-continuous stirred tank reactor, SSTR (cylindrical vessel of volume 1 L, diameter D_R = 0.1 m; liquid level $H_L = D_R$; 4 baffles; mixer: 6-bladed Rushton turbine of diameter D_M = 0.04 m and thickness x = 1 mm). The gas phase was introduced and discharged continuously. From the liquid and solid phases viewpoint the reactor was operated batchwise. The reactor was equipped with thermocouple, pH-control, the stirring frequency control, pressure sensor and polarographic oxygen probe for monitoring the oxygen concentration in the liquid phase. Ranges of reaction conditions are listed in Table 2. Kinetics of the model reaction was studied in the kinetics regime – influence of internal and external mass transfer was negligible (see [29] for evidence). Properties of the Pd/C catalyst used in this study are summarized in Table 3.

Table 2
Experimental conditions.

Condition	Range
Initial glucose concentration (mol m^{-3})	10–130
Initial gluconic acid concentration (mol m^{-3})	0–20
Oxygen partial pressure (kPa)	21–101
Total pressure (kPa)	101
Temperature (K)	303
pH	8.1
Stirring frequency (min^{-1})	600
Catalyst particle size (μm)	45

Table 3
Characteristics of the Pd/C catalyst.

Property	Value
Code	Cherox 41-00
Support	Activated carbon Supersorbon HB-3
Specific Pd content ($mol_{Pd}\ kg_{cat}^{-1}$)	0.2631
Specific Pd content ($\%_w$)	2.8
Porosity	0.695
Apparent density ($kg\ dm^{-3}$)	0.6743
True density ($kg\ dm^{-3}$)	2.212
S_{BET} ($m^2\ g^{-1}$)	1328.5 (total); 871.8 (micropores)

The glucose oxidation produces gluconic acid which lowers pH of the reaction mixture and decreases the catalyst activity during operation. Therefore, pH was set to value 8.1 and kept constant by addition of concentrated NaOH solution. Change of the reaction mixture volume due to addition of NaOH solution did not exceed 1%, and was therefore neglected. The reactor operated at low Glc conversion, up to 10%, so that according to Kunz and Recker [5] assumption of 100% selectivity towards Glcac could be taken. Consumption of NaOH during reaction yielded information about the amount of Glcac formed.

Rate of Glcac formation in the batch reactor without change in volume of the liquid phase is defined as follows:

$$R_{w,Glcac} = \sum_j \nu_{j,Glcac}\dot{\xi}_{w,j} = \frac{dc_{Glcac}}{\rho_c dt} \tag{17}$$

The Glcac concentration derivative term in Eq. (17) was obtained after differentiating power function (18) that was used to fit the concentration–time data.

$$y = y_0 + ax^b \tag{18}$$

The form of function (18) made it possible to easily find time t_0 of the reaction start-up (by expressing x for $y = 0$). This time corresponds with the initial rate of Glcac formation, $R^0_{w,Glcac}$.

3.2. Experimental procedure

Before each experiment the catalyst was activated in the reactor by reduction under inert atmosphere with Glc, which was a component of the reaction mixture. Existence of optimum in activation time was observed and put in correlation with the Glc concentration in the reactor, see [29]. The reaction was started up by replacing nitrogen flow with flow of nitrogen/oxygen mixture of desired partial pressure of oxygen. Each experiment consisted of one or more consecutive oxidation runs of cca. 5200 s. Between two consecutive oxidation runs the catalyst was reactivated in inert atmosphere by Glc (see Fig. 1 for illustration).

4. Results and discussion

4.1. The kinetics model parameters estimation

Several possible mechanistic variations describing the catalytic glucose oxidation were considered in formulation of a kinetic model. The kinetic model determined by Eqs. (1) and (2) emerges from the mechanism summarized in Table 1. It was selected by best fitting the experimental data. Parameters of the proposed kinetics model (Eqs. (1) and (2)) are listed in Table 4. They were calculated by using Era 3.0 software [30] for regression analysis. The objective function took form of sum of weighted squared differences between

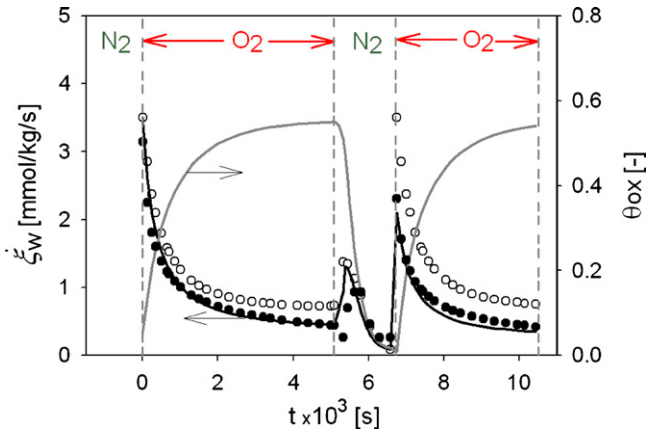

Fig. 1. Transient reaction rate and extent of the catalyst deactivation (represented by θ_{so}) during Glc oxidation in SSTR. Primary experimental data (●); data recalculated for concentrations at the reaction start-up (○); lines, the kinetic model solution. Experimental conditions: SSTR; $c^0_{Glc} = 100\ mol\ m^{-3}$; $c^0_{Glcac} = 0\ mol\ m^{-3}$; $\rho_c = 1\ kg\ m^{-3}$; $p(O_2) = 101\ kPa$; $T = 303\ K$; pH = 8.1.

observed and predicted values of dependent variables:

$$F = \sum_{j=1}^{Ne}\sum_{i=1}^{Ny} w_{ij}\left(y_{ij}^{observed} - y_{ij}^{predicted}\right)^2 = \min \tag{19}$$

In Eq. (19) Ne denotes the number of experimental data points, Ny number of dependent variables, $y = c_{Glc}$, c_{Glcac}, c_O, θ_{so}. The weight coefficient, w_{ij}, is defined as follows:

$$w_{ij} = \frac{1}{\max(|y_{ij}^{observed}|, \varepsilon)} \tag{20}$$

where $\varepsilon = 1 \times 10^{-10}$. See [30] for more computational details on Era 3.0.

Based on the proposed mechanism (Table 1), term $K_3K_1c_{Glc}$ was supposed to appear in denominator of the rate equation. It was neglected for its low value.

Eqs. (1) and (2) mathematically describe processes of the main surface reaction, the catalyst deactivation and the catalyst reactivation. The mechanism presented in Table 1 applies all the time except when oxygen concentration in the liquid phase approaches zero. Then the mechanism changes: inactive oxygen species (responsible for the catalyst deactivation) take over the function of the chemisorbed oxygen in the main surface reaction. When the mechanism changes, its mathematical description also changes, and Eqs. (21) and (22) apply as the kinetics model instead of Eqs. (1) and (2). Gangwal et al. [31] declares having avoided reconstruction of their kinetics model under these conditions.

$$\dot{\xi}_w = k_w^+ c_{Glc}\theta_{so}(1 - \theta_{so}) \tag{21}$$

$$\frac{d\theta_{so}}{dt} = \rho_c V_L k_A \theta_{so}(1 - \theta_{so}) \tag{22}$$

where $k_w^+ = 5.47 \times 10^{-5}\ m^3\ kg^{-1}\ s^{-1}$.

Table 4
Parameters of Eqs. (1) and (2).

Rate and adsorption constant	Dimension	Value	Std Error
$k_w = k_{w,4}C_{p,tot}C_{ch,tot}{}^2K_1K_3K_2$	$[m^{4.5}\ kg^{-1}\ mol^{-0.5}\ s^{-1}]$	0.00313	0.00004
$K_{Glc} = K_1$	$[m^3\ mol^{-1}]$	0.0169	0.0004
$K_O = K_2$	$[m^{1.5}\ mol^{-0.5}]$	4.50	0.01
$K_{Glcac} = K_5/c_{OH-}$	$[m^3\ mol^{-1}]$	0.384	0.009
$k_D = k_{w,6}C_{ch,tot}C_{x,tot}K_2$	$[m^{1.5}\ mol^{-0.5}\ kg^{-1}\ s^{-1}]$	0.00612	0.0002
$k_A = k_{w,7}C_{ch,tot}{}^2$	$[kg^{-1}\ s^{-1}]$	0.00518	0.0002

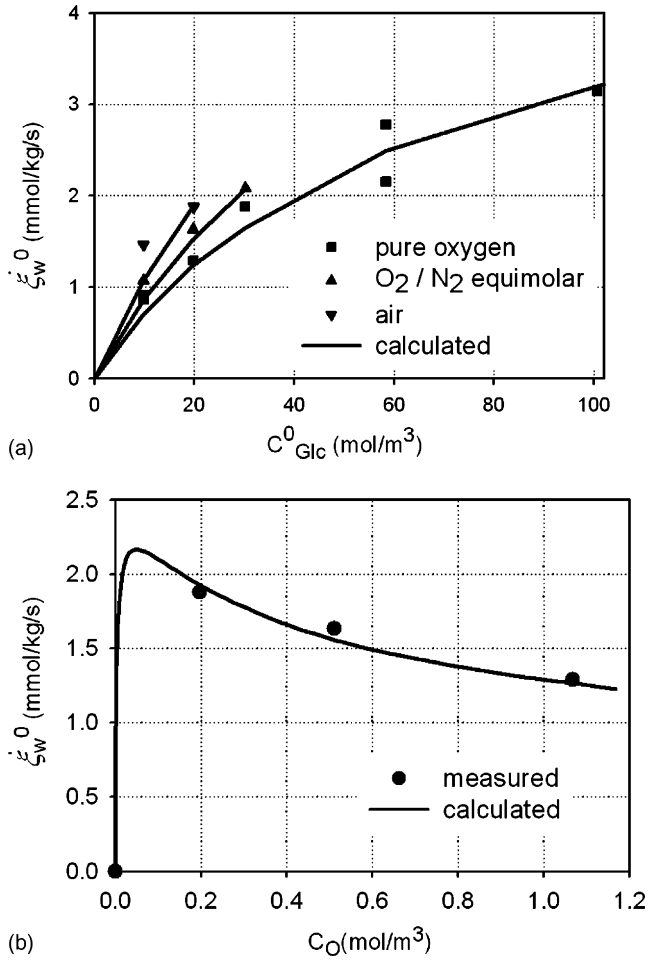

Fig. 2. Initial reaction rate as a function of (a) Glc initial concentration, and (b) oxygen concentration in bulk liquid. Dots, measured; lines, solution of the kinetic model. Experimental conditions: SSTR; $c^0_{Glcac} = 0.5$ mol m^{-3}; $\rho_c = 1$ kg m^{-3}; $T = 303$ K; pH = 8.1; (b) $c^0_{Glc} = 20$ mol m^{-3}.

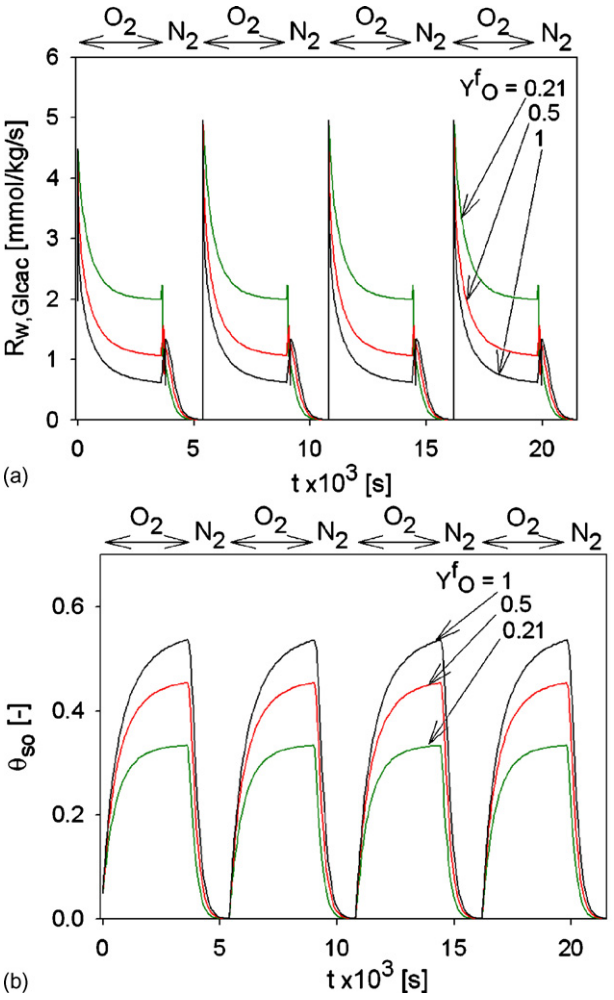

Fig. 3. Simulations of four reaction cycles in CSTR operating in periodic O_2/N_2 mode for various oxygen molar fractions in the gas feed stream. Time course of (a) immediate rate of Glcac formation, (b) the catalyst fractional coverage by inactive oxygen species. Conditions: $t_R = 3600$ s; $t_A = 1800$ s; $\rho_c = 1$ kg m^{-3}; $V_R = 860$ cm^3; c_{Glc} = const.; $X_{Glc} = 2\%$; $c^f_{Glc} = 100$ mol m^{-3}; $c^f_{Glcac} = 0$.

4.2. Effect of the reagents concentrations

Fig. 1 shows record of a representative experiment. Good agreement was achieved between measured (dots in Fig. 1) and calculated (lines in Fig. 1) processes of Glc oxidation and the catalyst reactivation.

In Fig. 1 a short period of the reaction rate elevation is observable after O_2 in the SSTR gas feed stream is replaced with N_2, at the beginning of the reactivation process. Concentration of oxygen dissolved in the liquid phase and that adsorbed on the catalyst surface is decreasing. During this period of time, kinetic aspects explained with Fig. 2b apply. Therefore, the reaction rate temporarily increases while the oxygen concentration decreases. After the oxygen concentration gets too low, only the inactive oxygen species take part in the main reaction. This period is no longer related with Fig. 2b.

The reaction rate at the beginning of the second reaction cycle (Fig. 1) is lower because the reaction mixture composition changed during the first reaction cycle in the batch system (SSTR). To prove full reversibility of the catalyst deactivation, the primary experimental data in Fig. 1 were corrected for the change in the reaction mixture composition (empty circles in Fig. 1). Glc and Glcac concentrations at the reaction start-up were applied in kinetic equation of Glc oxidation to serve this purpose. The full reversibility of the Pd/C catalyst deactivation is in agreement with similar findings of Vleeming et al. for the case of Pt catalyst [3].

Fig. 2 shows effects of the reagents' initial concentration on the initial reaction rate in SSTR. Limitation in the range of experimental conditions in Fig. 2a was enforced by satisfying the condition of negligible external diffusion influence on the overall reaction rate (see [29] for evidence that the kinetics regime was obeyed). Fig. 2b indicates that the Glc oxidation is significantly inhibited by oxygen. The reaction rate is accelerated at low oxygen concentrations. It is also retarded on raising the Glcac initial concentration. Glucose has positive effect on the reaction rate as can be seen in Fig. 2a. The observations summarized in Fig. 2 are in agreement with similar experiments published earlier [3].

Acceleration of the reaction rate by decreasing oxygen concentration demonstrated in Fig. 2, can partly be ascribed to somewhat higher value of the oxygen adsorption constant (see K_O value in Table 4). It suggests strong adsorption of oxygen on the catalyst surface. On the other hand, as will be demonstrated in the next section (and Fig. 3b), raising the oxygen concentration in the liquid phase brings about higher formation of the inactive oxygen species responsible for the catalyst deactivation.

4.3. CSTR operating in periodic mode

The above-indicated possibility of improving the reactor performance by exchanging the reaction and reactivation cycles was

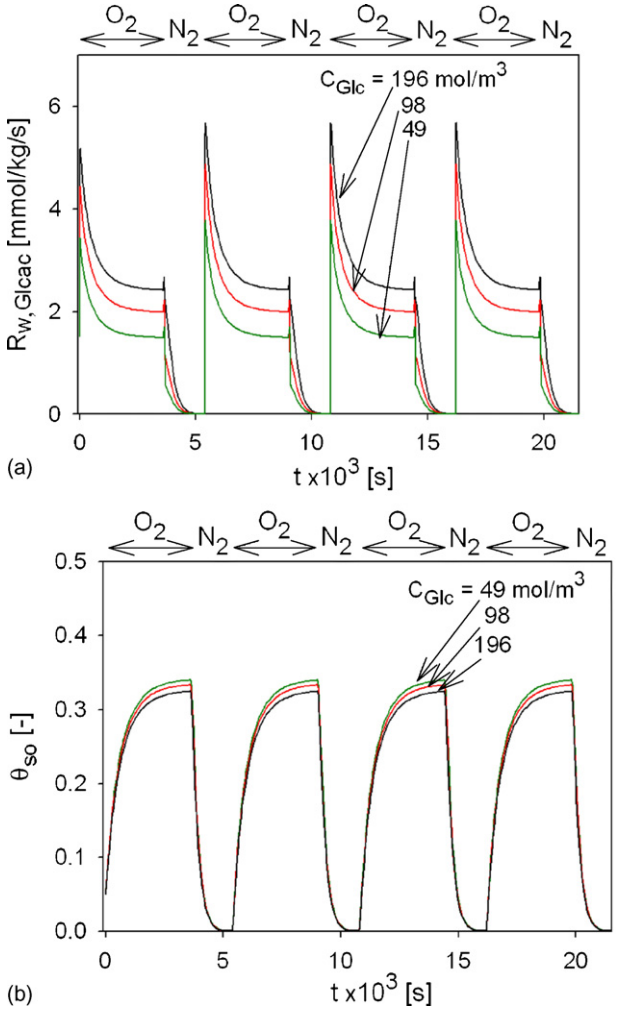

Fig. 4. Simulations of four reaction cycles in CSTR operating in periodic O_2/N_2 mode for various Glc concentrations in the reaction mixture. Time course of (a) immediate rate of Glcac formation, (b) the catalyst fractional coverage by inactive oxygen species. Conditions: $t_R = 3600$ s; $t_A = 1800$ s; $\rho_c = 1$ kg m^{-3}; $V_R = 860$ cm^3; c_{Glc} = const.; $X_{Glc} = 2\%$; $Y^f_O = 0.21$; $c^f_{Glcac} = 0$.

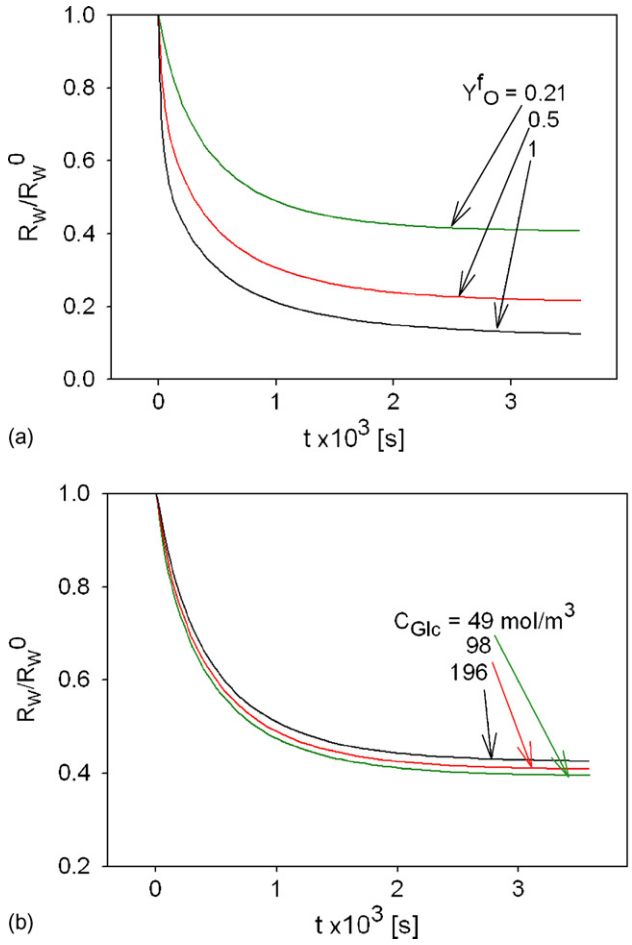

Fig. 5. Time course of the catalyst activity, expressed through ratio of the immediate to the initial rate of Glcac formation in CSTR as a function of (a) oxygen molar fraction in the gas feed stream, (b) Glc concentration in the reaction mixture. The case "(a)" corresponds to the conditions of the second reaction cycle of Fig. 3; the case "(b)" to similar conditions of Fig. 4.

examined further. For deeper insight into the model system under periodic mode of operation, the SSTR model (Eqs. (9)–(13)) was modified for conditions of CSTR operating at constant Glc and Glcac concentrations in time and varying volumetric flow rate of the liquid feed stream according to the actual reaction rate. Results of this approach are presented in Figs. 3–5.

In the kinetics model (Eqs. (1) and (2)), the change in the catalyst activity is expressed through the change in the fractional coverage by inactive oxygen species, θ_{so}. Relation between θ_{so} and the activity is given in Eq. (7).

The CSTR application of the kinetics model enables, in contrast with the SSTR one, to separate the effect of the reagents concentrations from the effect of the change in the catalyst activity itself on deviation of the reaction rate in time. Thus, it makes the study of the deactivating reaction system more transparent. The CSTR model makes it possible to express the catalyst activity directly through the ratio of the immediate to the initial reaction rate (i.e. by using Eq. (4)), and reveals directly the progress in the extent of the catalyst deactivation. This approach is for the cases of the second reaction cycle of Figs. 3 and 4 depicted in Fig. 5.

Comparison of Figs. 3b and 4b with 5a and b, respectively, leads through Eq. (7). The rate and the extent of the catalyst deactivation are definitely influenced by oxygen concentration in the liquid phase. With its raise, both the θ_{so} steady-state value as well as the transient one increase (Fig. 3b), and the catalyst's transient and steady-state activity decreases (Fig. 5a). On the contrary, unimportant is the effect of Glc concentration in the reaction mixture on the catalyst deactivation extent (Figs. 4b and/or 5b).

4.4. Optimization of the CSTR productivity

This section deals again with CSTR running at constant Glc and Glcac concentrations in time and varying the volumetric flow rate of the liquid feed stream according to the actual reaction rate. CSTR of this section differs in the way of the gas feed flow modulation. The reactor is now operated under on–off periodic mode, i.e. with alternating cycles of switching on and off air feed stream. The catalyst reactivation in this case runs without assistance of nitrogen. Fig. 6a shows course of the model reaction cycle-time-averaged reaction rate as a function of the period length and split value. The period length is defined as a sum of reaction and reactivation times ($P = t_R + t_A$). The split of period is the time the reaction takes in relation to the entire period length ($S = t_R/(t_R + t_A)$). As can be seen in Fig. 6a, for any period length always a split value exists, where maximum reaction rate is achieved. The reaction rate is cycle-time-averaged and represents the reactor productivity.

The optimization task was to find conditions that guarantee the highest reactor productivity at any period given. In other words, the goal was to share optimally the reaction and reactivation times

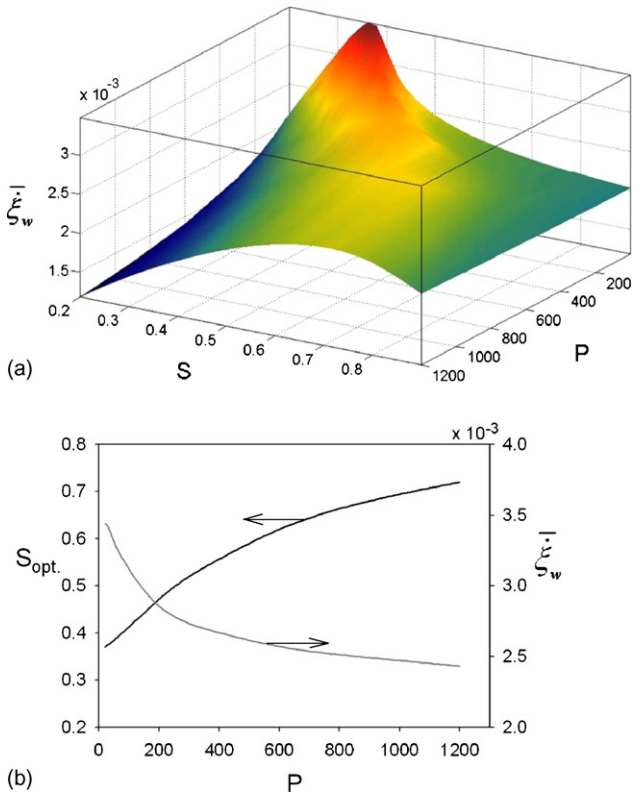

Fig. 6. Simulation of the model reaction run in CSTR operated under on–off periodic mode, i.e. with alternating cycles of switching on and off air feed stream. (a) Cycle-time-averaged reaction rate as a function of period length and split value. (b) Trajectory of the maximum reactor productivity retrieved from the graph "(a)". (The model solution is not credible in $P \rightarrow 0$, see the text). Conditions: $\rho_c = 1\ \mathrm{kg\,m^{-3}}$; $V_R = 860\ \mathrm{cm^3}$; $Y_O^f = 0.21$; $c_{Glcac}^f = 0$; $X_{Glc} = 2\%$; $c_{Glc}^f = 100\ \mathrm{mol\,m^{-3}}$.

within given period length, so that neither any time is wasted in prolonged activation process, nor an insufficient activation time is provided. The reactor productivity would drop down in both of these cases. Fig. 6 maps the reactor performance for selected input conditions. For illustration, the trajectory of the maximum reactor productivity is retrieved from Fig. 6a and highlighted in Fig. 6b.

As the period length stretches, in Fig. 6b, the optimal split shifts upwards (i.e. the reaction time raises). At the same time, depression in the cycle-time-averaged reaction rate (which still is the highest possible one for the period given, see Fig. 6a) occurs as a consequence of a shift in deactivation extent of the catalyst after accomplishing the reaction time portion of the whole period time given.

In the direction of decreasing the values of P and S in Fig. 6a, the system approaches operation of such a hypothetical CSTR that runs without the periodic on–off mode, but with lower content of oxygen in gas feed stream (compared to oxygen content in the on-mode of the original system). In the opposite direction the system approaches operation of such CSTR that runs without reactivation of the catalyst and the cycle-time-averaged reaction rate approaches value of steady-state reaction rate of such system. It should be noted that the model solution in Fig. 6 ought to be "taken with a pinch of salt" in the region near $P = 0$. A relation between the gas flow rate to the reactor and the gas holdup in it becomes important in this region. The model does not take it into account.

5. Outlooks and recommendations

The goal of this study was not to declare the "best periodic operation", as it differs with the input conditions and with the operational requirements and limitations. The goal was to find the trajectory of the maximum reactor performance for given input conditions. A real plant operational requirements and limitations would decide about the position on this trajectory then. This is the guideline to follow at optimizing the intended gas-lift reactor operation (see next).

The reaction rate is accelerated at low oxygen concentration. Further decrease in oxygen concentration can be achieved when external diffusion plays a role. The model system can be carried out in diffusion regime and under periodic mode, at the same time, in gas-lift reactor (GLR). In principle, the GLR natural operation resembles the above described forced periodic operation of CSTR as follows: in the riser section of the GLR air is introduced. This section serves then as the reaction zone and the oxidation reaction along with the catalyst deactivation occurs here. If complete separation of the gas is ensured in separator of the reactor, downcomer section of the GLR serves as the catalyst reactivation zone. In GLR, the period length is set by the liquid circulation velocity. Split of the period is set by residence times in the GLR individual sections. Preliminary results on design of GLR suited for the model process were presented by the authors [32,33].

In the experimental SSTR, the model reaction kinetics was studied under transient conditions in kinetic regime. State-of-the-art transient techniques to study catalysts and their performance are reviewed by Berger et al. [34]. They enable better determination of a reaction mechanism and are therefore valuable at prediction intrinsic processes with cyclic exposure of a catalyst to different conditions. It is believed that in non-steady-state each step of the reaction mechanism proceeds at its own pace and according to its own kinetic nature. This approach, however, leads to the solution of robust mathematical framework to obtain the kinetics parameters. In this study, simplification was made by assuming the rate limiting step in the reaction mechanism (LHHW kinetics of Table 1). On the other hand, existence of a rate limiting step is questionable under transient operation of a catalyst [35]. Impact of the dynamic phenomena on optimization of the CSTR operation would be useful theme for next research.

6. Conclusions

Optimization of the CSTR productivity through the gas feed flow modulation was attempted. The task was to share optimally the reaction and reactivation times within given period length, so that neither any time is wasted in prolonged activation process, nor an insufficient activation time is provided. In the periodic operation, enhancement of the overall reaction rate results from forcing the catalyst to operate under transient conditions. In the optimal periodic operation the catalyst cycle-time-averaged activity was long-term-steady. Mathematical model of CSTR operating under on-off periodic mode was used to aid the optimization task. Fig. 6 maps the reactor productivity for chosen input operational conditions. Trajectory of the highest possible reactor productivity for these input conditions was found.

Kinetics of glucose oxidation in liquid phase over Pd/C was studied and discussed to facilitate the above mentioned optimization study. Kinetics model was formulated to adequately describe the model reaction kinetics including the catalyst deactivation and reactivation. The deactivation due to the action of oxygen during the model reaction course is fully reversible (as explained with Fig. 1). Glc oxidation is significantly inhibited by oxygen. It was found that raising the oxygen concentration in the liquid phase brings about higher formation of the inactive oxygen species responsible for the catalyst deactivation. Figs. 3b and 5a show that the higher is the oxygen concentration, the faster and more profound the catalyst deactivation gets. On the other hand, Glc concentration in the

reaction mixture has negligible effect on the catalyst deactivation extent.

Acknowledgements

We acknowledge financial support of Grant Agency of the Czech Republic (grant no.: 203/08/H032). Our thanks go to Prof. Jozef Markoš from Slovak University of Technology in Bratislava for reading the manuscript and providing valuable feedback.

References

[1] I. Nikov, K. Paev, Palladium on alumina catalyst for glucose oxidation: reaction kinetics and catalyst deactivation, Catal. Today 24 (1995) 41–47.
[2] A.P. Markusse, B.F.M. Kuster, J.C. Schouten, Platinum catalysed aqueous methyl-a-D-glucopyranoside oxidation in a multiphase redox-cycle reactor, Catal. Today 66 (2001) 191–197.
[3] J.H. Vleeming, B.F.M. Kuster, G.B. Marin, Selective oxidation of methyl α-D-glucopyranoside with oxygen over supported platinum: kinetic modeling in the presence of deactivation by overoxidation of the catalyst, Ind. Eng. Chem. Res. 36 (1997) 3541–3553.
[4] T. Mallat, A. Baiker, Oxidation of alcohols with molecular oxygen on platinum metal catalysts in aqueous solutions, Catal. Today 19 (1994) 247–284.
[5] M. Kunz, C. Recker, A new continuous oxidation process for carbohydrates, Carbohydr. Eur. 13 (1995) 11–15.
[6] A. Mirescu, U. Prusse, A new environmental friendly method for the preparation of sugar acids via catalytic oxidation on gold catalyst, Appl. Catal. B: Environ. 70 (2007) 644–652.
[7] N. Thielecke, K.D. Vorlop, U. Prusse, Long-term stability of an Au/Al_2O_3 catalyst prepared by incipient wetness in continuous-flow glucose oxidation, Catal. Today 122 (2007) 266–269.
[8] S. Biella, L. Prati, M. Rossi, Selective oxidation of D-glucose on gold catalyst, J. Catal. 206 (2002) 242–247.
[9] J. Klein, M. Rosenberg, J. Markoš, O. Dolgoš, M. Krošlák, Ľ. Krištofíková, Biotransformation of glucose to gluconic acid by *Aspergillus niger*—study of mass transfer in an airlift bioreactor, Biochem. Eng. J. 10 (3) (2002) 195–205.
[10] M. Juraščík, M. Hucík, I. Sikula, J. Annus, J. Markoš, Influence of biomass on hydrodynamics of an internal loop airlift reactor, Chem. Pap. 60 (6) (2006) 441–445.
[11] O.V. Singh, R. Kumar, Biotechnological production of gluconic acid: future implications, Appl. Microbiol. Biotechnol. 75 (2007) 713–722.
[12] I. Sikula, M. Juraščík, J. Markoš, Modeling of fermentation in an internal loop airlift bioreactor, Chem. Eng. Sci. 62 (2007) 5216–5221.
[13] J. Liu, Z. Cui, Optimization of operating conditions for glucose oxidation in an enzymatic membrane bioreactor, J. Membr. Sci. 302 (2007) 180–187.
[14] I. Sikula, J. Markoš, Modeling of enzymatic reaction in an airlift reactor using an axial dispersion model, Chem. Pap. 62 (1) (2008) 10–17.
[15] G. Ketteler, D.F. Ogletree, H. Bluhm, H. Liu, E.L.D. Hebenstreit, M. Salmeron, In situ spectroscopic study of the oxidation and reduction of Pd(1 1 1), J. Am. Chem. Soc. 127 (2005) 18269–18273.
[16] G.W. Simmons, Y. Wang, J. Marcos, K. Klier, Oxygen adsorption on Pd(1 0 0) surface: phase transformations and surface reconstruction, J. Phys. Chem. 95 (1991) 4522–4528.
[17] E. Lundgren, G. Kresse, C. Klein, M. Borg, J.N. Andersen, M. De Santis, Y. Gauthier, C. Konvicka, M. Schmid, P. Varga, Two-dimensional oxide on Pd(1 1 1), Phys. Rev. Lett. 88 (24) (2002).
[18] P.L. Silveston, J. Hanika, Challenges for the periodic operation of trickle-bed catalytic reactors, Chem. Eng. Sci. 57 (2002) 3373–3385.
[19] P.L. Silveston, J. Hanika, Periodic operation of three-phase catalytic reactors, Can. J. Chem. Eng. 82 (2004) 1105–1142.
[20] J.G. Boelhouwer, H.W. Piepers, A.A.H. Drinkenburg, Advantages of forced non-steady operated trickle-bed reactors, Chem. Eng. Technol. 25 (2002) 647–650.
[21] V. Tukač, J. Hanika, V. Chyba, Periodic state of wet oxidation in trickle-bed reactor, Catal. Today 79–80 (2003) 427–431.
[22] G. Liu, X. Zhang, L. Wang, S. Zhang, Z. Mi, Unsteady-state operation of trickle-bed reactor for dicyclopentadiene hydrogenation, Chem. Eng. Sci. 63 (2008) 4991–5002.
[23] P.L. Silveston, Composition modulation of catalytic reactors, Gordon and Breach Science Publishers, 1998.
[24] S. Szépe, O. Levenspiel, Catalyst deactivation, in: Proceedings of the 4th European Symposium on Chemical Reaction Engineering, Oxford, 1970.
[25] J.B. Butt, E.E. Petersen, Activation, Deactivation and Poisoning of Catalysts, Academic Press, Inc., 1988.
[26] V. Linek, T. Moucha, J. Sinkule, Gas-liquid mass transfer in vessels stirred with multiple impellers. I. Gas–liquid mass transfer characteristics in individual stages, Chem. Eng. Sci. 51 (12) (1996) 3203–3212.
[27] W. Bujalski, A.W. Nienow, S. Chatwin, M. Cooke, The dependency on scale of power numbers of Rushton disc turbines, Chem. Eng. Sci. 42 (2) (1987) 317–326.
[28] H. Eya, K. Mishima, M. Nagatani, Y. Iwai, Y. Arai, Measurements and correlation of solubilities of oxygen in aqueous solutions containing glucose, sucrose and maltose, Fluid Phase Equilib. 94 (1994) 201–209.
[29] Z. Gogová, J. Hanika, Experimental study of palladium catalyst reactivation during glucose oxidation by molecular oxygen, Chemical Pap., 63 (2009), in press.
[30] P. Zámostný, Z. Bělohlav, A software for regression analysis of kinetic data, Comput. Chem. 23 (1999) 479.
[31] V.R. Gangwal, J. van der Schaaf, B.F.M. Kuster, J.C. Schouten, Noble-metal-catalysed aqueous alcohol oxidation: reaction start-up and catalyst deactivation and reactivation, J. Catal. 232 (2005) 432–443.
[32] Z. Gogová, J. Hanika, Purpose tailored design of gas-lift reactor, in: Proceedings of the 35th International Conference of SSCHE, Tatranské Matliare, Slovakia, 2008.
[33] Z. Gogová, J. Hanika, Model aided design of gas-lift reactor for oxidation reaction with fast reversible catalyst deactivation, in: Proceedings of the 10th international Chemical and Biochemical Conference Chempor 2008, Braga, Portugal, 2008.
[34] R.J. Berger, F. Kapteijn, J.A. Moulijn, G.B. Marin, J. De Wilde, M. Olea, D. Chen, A. Holmen, L. Lietti, E. Tronconi, Y. Schuurman, Dynamic methods for catalytic kinetics, Appl. Catal. A: Gen. 342 (1–2) (2008) 3–28.
[35] M. Pekař, J. Koubek, Rate-limiting step. Does it exist in the non-steady state? Chem. Eng. Sci. 52 (14) (1997) 2291–2297.